Superlattices and Microstructures 52 (2012) 1131–1142

Contents lists available at SciVerse ScienceDirect

Superlattices and Microstructures

journal homepage: www.elsevier.com/locate/superlattices

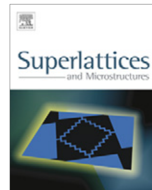

The structure and photocatalytic activity of TiO_2 thin films deposited by dc magnetron sputtering

W.J. Yang [a,f], C.Y. Hsu [b], Y.W. Liu [b], R.Q. Hsu [a], T.W. Lu [c,d], C.C. Hu [c,e,*]

[a] *Department of Mechanical Engineering, National Chiao Tung University, Hsinchu, Taiwan, ROC*
[b] *Department of Mechanical Engineering, Lunghwa University of Science and Technology, Taoyuan, Taiwan, ROC*
[c] *Institute of Biomedical Engineering, National Taiwan University, Taipei, Taiwan, ROC*
[d] *Department of Orthopaedic Surgery, School of Medicine, National Taiwan University, Taipei, Taiwan, ROC*
[e] *Department of Mechanical Engineering, Ming Chi University of Technology, Taipei, Taiwan, ROC*
[f] *Center for Thin Film Technologies and Applications, Ming Chi University of Technology, Taipei, Taiwan, ROC*

ARTICLE INFO

Article history:
Received 8 March 2012
Received in revised form 28 July 2012
Accepted 20 August 2012
Available online 11 September 2012

Keywords:
TiO_2 thin films
Photocatalytic activity
dc magnetron sputtering
Taguchi method

ABSTRACT

This paper seeks to determine the optimal settings for the deposition parameters, for TiO_2 thin film, prepared on non-alkali glass substrates, by direct current (dc) sputtering, using a ceramic TiO_2 target in an argon gas environment. An orthogonal array, the signal-to-noise ratio and analysis of variance are used to analyze the effect of the deposition parameters. Using the Taguchi method for design of a robust experiment, the interactions between factors are also investigated. The main deposition parameters, such as dc power (W), sputtering pressure (Pa), substrate temperature (°C) and deposition time (min), were optimized, with reference to the structure and photocatalytic characteristics of TiO_2. The results of this study show that substrate temperature and deposition time have the most significant effect on photocatalytic performance. For the optimal combination of deposition parameters, the (1 1 0) and (2 0 0) peaks of the rutile structure and the (2 0 0) peak of the anatase structure were observed, at $2\theta \sim 27.4°$, 39.2° and 48°, respectively. The experimental results illustrate that the Taguchi method allowed a suitable solution to the problem, with the minimum number of trials, compared to a full factorial design. The adhesion of the coatings was also measured and evaluated, via a scratch test. Superior wear behavior was observed, for the TiO_2 film, because of the increased strength of the interface of micro-blasted tools.

© 2012 Elsevier Ltd. All rights reserved.

* Corresponding author at: Department of Mechanical Engineering, Ming Chi University of Technology, Taipei, Taiwan, ROC. Tel.: +886 2 29089899; fax: +886 2 29063269.
E-mail address: cchu@mail.mcut.edu.tw (C.C. Hu).

0749-6036/$ - see front matter © 2012 Elsevier Ltd. All rights reserved.
http://dx.doi.org/10.1016/j.spmi.2012.08.013

1. Introduction

Because of their nontoxic nature, good stability, ease of mass production and high controllability, titanium dioxide (TiO_2) thin films are used, as a photocatalyst, in many fields, such as anti-fogging glasses, self-cleaning windows, easy-to-clean surfaces and water purification devices [1,2]. Of the four phases of TiO_2 films (amorphous, anatase, rutile and brookite), anatase TiO_2 is the most commonly used. In the photocatalytic process, the band-gap of TiO_2, of rutile tetragonal structure, is about 3.2 eV. It can be irradiated by illumination ultraviolet (UV) light, to perform inter-band transition [3]. The electron–hole pairs created in the transition create holes in the valence band and electrons in the conduction band. These holes generate hydroxyl radicals and the excited electrons generate super oxide anions, which turn organic pollutants into the harmless intermediate organic compounds, CO_2 and H_2O [4]. Several methods are used to fabricate TiO_2 thin films, including chemical vapor deposition, pulsed laser deposition, sol–gel processing and magnetron sputtering. Sol–gel processing is the most commonly used commercially, but the thickness of the TiO_2 films produced is not easy controlled and they exhibit poor adhesion [5]. The low-cost magnetron sputtering technique, used in the large-area fabrication industry is more controllable and is used in many photocatalytic applications [6–8]. Eufinger et al. studied the photocatalytic activity of amorphous TiO_2 thin films, deposited using dc magnetron sputtering [9]. Šícha et al. studied the structural behavior of photocatalytic TiO_2 films, sputtered at temperatures below 200 °C [10]. Sung and Kim studied the surface treatment of TiO_2 films, for use in dye-sensitized solar cells [11]. Lin et al. examined the crystalline structure, surface morphology and photocatalytic activity of the TiO_2 films were affected by oxygen partial pressure flow rate ratios [12]. Liu et al. studied the effect of oxygen partial pressure on the structure, surface morphology and photocatalytic properties of TiO_2 film [13]. This study examines the influence of various deposition process parameters on the photocatalytic activity of TiO_2 thin films grown on non-alkali glass ($25 \times 25 \times 1$ mm^3) substrates, by means of dc magnetron sputtering, with the aim of achieving a high deposition rate, low methylene blue (MB) absorbance and good hydrophilicity.

The Taguchi method is a systematic method for the design and analysis of experiments, which can be used to design low-cost products, with improved quality [14]. To optimize the deposition process for TiO_2 photocatalyst films, using experimental data, a traditional statistical regression requires a large amount of data, which creates difficulty in treating the typical normal distribution of data, because of a lack of variable factors [15]. A statistical analysis of signal-to-noise ratio (S/N) was performed, using analysis of variance (ANOVA). The optimal deposition parameters were obtained, by analyzing the experimental results for various experimental permutations [16]. Table 1 demonstrates the impact of four deposition parameters, at three levels on the quality of TiO_2 photocatalyst films; these are dc power, sputtering pressure, substrate temperature and deposition time. An L_9 (3^4, with four columns and nine rows) orthogonal array was employed.

2. Experimental procedures

TiO_2 photocatalyst thin films were coated onto non-alkali glass substrates, using dc magnetron sputtering, in an Ar gas atmosphere. A 99.995% purity ceramic TiO_2 target was pre-sputtered, for 10 min, to remove contamination. The substrates were cleaned, in acetone, using ultrasound, rinsed with deionized water and dried in nitrogen. A vacuum, of base pressure, 6.0×10^{-4} Pa, was applied, before deposition. A constant distance between the substrate and the target (80 mm) and rotational speed of the substrate (10 rpm) were maintained. By adjusting the experimental permutations, this study examined the effect of each deposition parameter on the deposition rate, MB absorbance, contact angle to a pure water droplet, surface morphology and crystal structure.

A field emission scanning electron microscope (SEM, JEOL, JSM-6500F) analyzed the surface morphologies and an atomic force microscope (AFM, PSIA-XE-100) obtained topographical images. The structural properties were investigated by X-ray diffraction (Rigaku-2000 X-ray Generator), using Cu Kα radiation (40 kV, 30 mA and $\lambda = 0.1541$ nm), with a grazing incidence angle of 1°; the scanning

Table 1
Deposition conditions, for TiO_2 thin films; factors and levels.

Substrate		Non-alkali glass; 25 × 25 × 1 mm^3		
Target		TiO_2; 99.995% purity; 50.8 mm diameter		
Gas		Argon (99.995%)		
Base pressure		6.0×10^{-4} Pa		
Substrate rotate vertical axis		10 rpm		
Substrate-to-target distance		80 mm		
Symbol	Process parameter	Level 1	Level 2	Level 3
A	Dc power (W)	90	120	150
B	Sputtering pressure (Pa)	1	1.5	2
C	Substrate temperature (°C)	300	400	500
D	Deposition time (min)	60	120	180

rate was 5°/min. A surface profiler (α-step, Dektat 2) measured the film thickness, to evaluate deposition rates.

12 μmol Methylene Blue (MB) aqueous solution was photocatalyzed, in a quartz cell, at room temperature. TiO_2 film immersed in the solution was irradiated by a UVP UVL-225D lamp. A UV/Vis/NIR spectrometer (Jasco V-670) was used to measure the absorption spectra of the MB solution, as a function of the UV irradiation time, at 365 nm. The photoinduced hydrophilicity was estimated by measuring the contact angle to pure water, at room temperature, in ambient atmosphere, using a contact angle measuring system (FACE CA-VP150) with an experimental error of less than 1°. A black light (UVP UVL-225D) lamp, of main wavelength, 365 nm (1.5 mW/cm^2 at the film surface), was the UV light source. The film adhesion and stability were determined, using a scratch test.

3. Results and discussion

Oxide targets can be used in dc operated magnetrons, provided they are reasonably electrically conducting [17]. The TiO_2 ceramic target was an semiconductor having a sufficient conductivity of approximately 0.3 Ω-cm as a target for dc sputtering [18]. The dc magnetron sputtering from TiO_2 ceramic targets can be readily controlled and the deposited layers show good adhesion as well as good coating uniformity [19]. Table 2a shows the experimental signal–noise ratios (*S*/*N*), for deposition rates. The sputtering process parameter set, $A_3B_1C_3D_2$ (No.7), produces the best deposition rate of the nine experiments, with an average 5.85 nm/min. Table 2b shows the ANOVA results, which show that dc sputtering power has the dominant effect on the deposition rates, with a contribution ratio of 76.05%, followed by sputtering pressure, with a contribution ratio of 19.76%. Fig. 1 shows the *S*/*N* graph for the deposition rates. Deposition rate increases, as dc power is increased and the number

Table 2a
Experimental results for the deposition rates and *S*/*N* ratio.

No.	Control factors				Deposition rates (nm/min)		*S*/*N* (dB)
	A	B	C	D	D1	D2	
1	1	1	1	1	3.08	3.14	9.85
2	1	2	2	2	2.19	2.17	6.76
3	1	3	3	3	2.45	2.41	7.71
4	2	1	2	3	4.56	4.58	13.19
5	2	2	3	1	3.91	3.99	11.93
6	2	3	1	2	3.12	3.06	9.79
7	3	1	3	2	5.86	5.84	15.34
8	3	2	1	3	4.92	4.94	13.85
9	3	3	2	1	4.12	4.08	12.25

Table 2b
ANOVA results, for deposition rates.

Factor	Degree of freedom	Sum of square	Variance	Contribution (%)
A	2	49.7637	24.8818	76.05
B	2	12.9279	6.4639	19.76
C	2	1.2753	0.6376	1.95
D	2	1.4694	0.7347	2.24
Total	8	65.4480		100

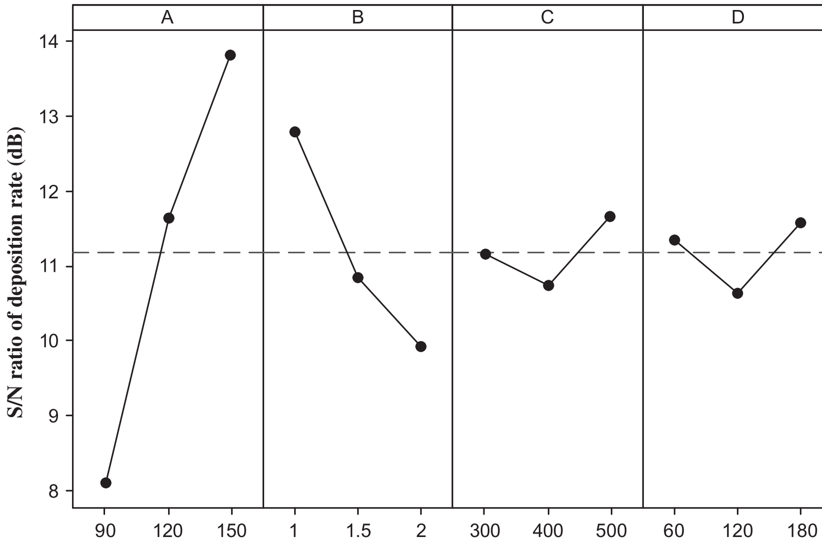

Fig. 1. *S*/*N* response graph, for deposition rates. (Note: A: dc power (W), B: sputtering pressure (Pa), C: substrate temperature (°C), D: deposition time (min).)

Table 3a
Experimental results, for MB absorbance and *S*/*N* ratio.

No.	Control factors				MB absorbance		*S*/*N* (dB)
	A	B	C	D	M1	M2	
1	1	1	1	1	0.712	0.717	2.92
2	1	2	2	2	0.465	0.4669	6.63
3	1	3	3	3	0.271	0.269	11.37
4	2	1	2	3	0.431	0.432	7.31
5	2	2	3	1	0.419	0.417	7.58
6	2	3	1	2	0.595	0.597	4.50
7	3	1	3	2	0.436	0.431	7.26
8	3	2	1	3	0.489	0.489	6.21
9	3	3	2	1	0.53	0.53	5.51

Table 3b
ANOVA results, for MB absorbance.

Factor	Degree of freedom	Sum of square	Variance	Contribution (%)
A	2	0.7017	0.3508	1.60
B	2	2.7560	1.3780	6.27
C	2	26.4277	13.2139	60.12
D	2	14.0740	7.0370	32.01
Total	8	43.9594		100

Table 3c
S/N response table, for MB absorbance.

Level	A	B	C	D
1	6.975	5.827	4.543	5.337
2	6.457	6.808	6.483	6.130
3	6.330	7.127	8.736	8.296
Effect	0.646	1.301	4.194	2.959
Rank	4	3	1	2

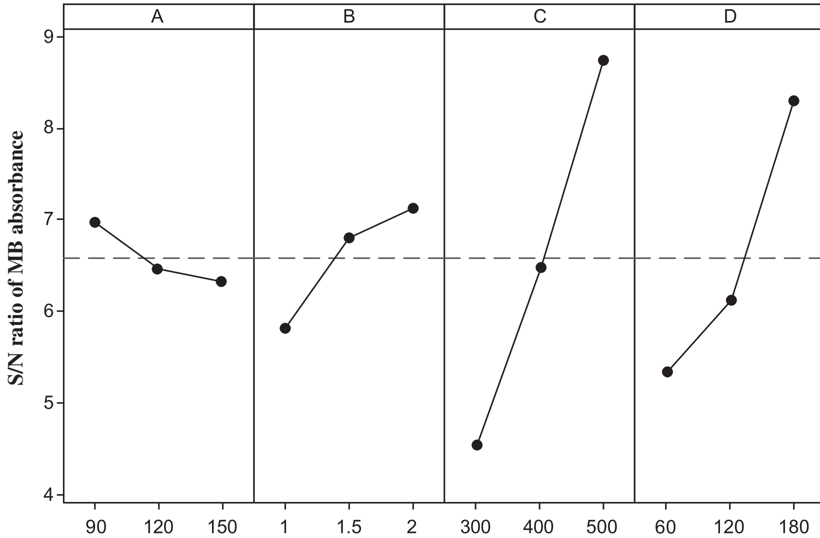

Fig. 2. *S/N* response graph, for MB absorbance.

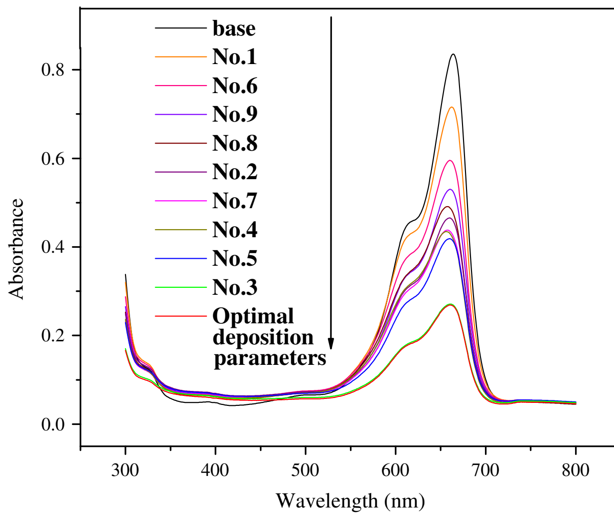

Fig. 3. Absorbance spectrum of MB aqueous solution (12 μmol), degraded using TiO_2 film, for orthogonal arrays No. 1–9, and the optimal deposition parameters ($A_1B_3C_3D_3$), for 4 h of UV irradiation.

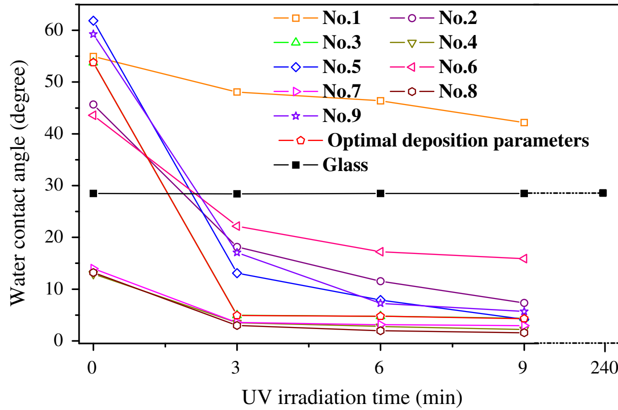

Fig. 4. The contact angles to pure water droplets during irradiation with UV irradiation.

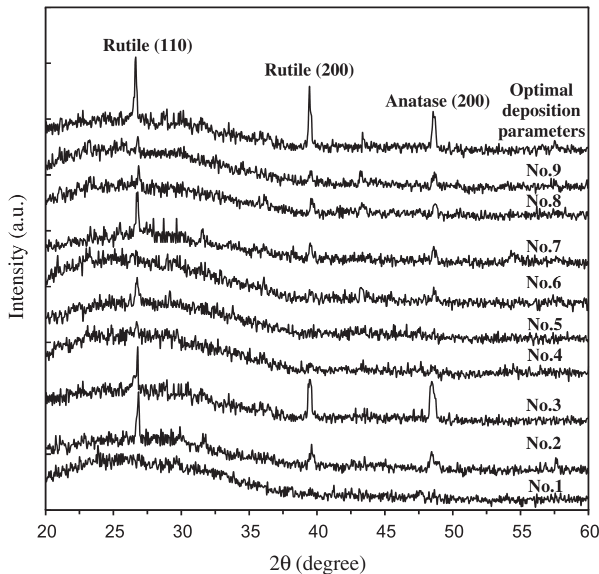

Fig. 5. XRD diffraction patterns of the TiO_2 films deposited with various sputtering parameters.

of atoms sputtered from the target is almost proportional to the power [20]. The higher the dc power, the more energy is received by the sputtered species and the greater is the film growth.

Table 3a lists the experimental results of MB absorbance and their signal–noise ratios (*S*/*N*). The TiO_2 film, with a sputtering process parameter set, $A_1B_3C_3D_3$ (No. 3), irradiated by UV light, exhibits the lowest MB absorbance characteristics of the nine experiments. Table 3b shows the ANOVA results, which show that the substrate temperature and the deposition time have the dominant effect on the MB absorbance, with a contribution ratio of almost 60.12% and 32.01%, respectively. The *S*/*N* response graphs are shown in Fig. 2. It can be seen that the *S*/*N* response for the MB absorbance increases, when the substrate temperature and the deposition time are increased (Table 3c).

Based on the analysis of *S*/*N* ratio, the deposition parameters that produce optimal MB absorbance, in TiO_2 photocatalyst films, are 90 W dc power (Level 1), 2 Pa sputtering pressure (Level 3), 500 °C

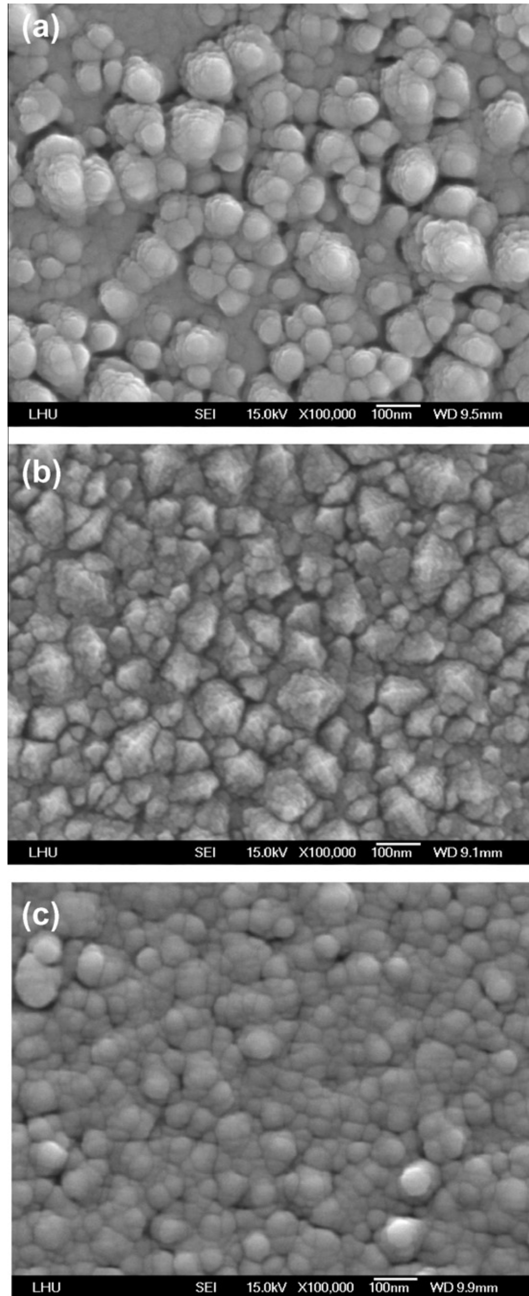

Fig. 6. SEM micrographs of TiO_2 films with different sputtering process parameters (a) $A_2B_1C_2D_3$, thickness = 822.6 nm, (b) $A_3B_1C_3D_2$, thickness = 702.0 nm, (c) $A_1B_3C_3D_3$ (optimal deposition condition), thickness = 437.4 nm, respectively.

substrate temperature (Level 3) and 180 min deposition time (Level 3). To validate these findings, a confirmation experiment was conducted, using the optimal levels for the deposition parameters, $A_1B_3C_3D_3$ (orthogonal array parameters No. 3). Fig. 3 shows the absorption spectra of MB aqueous

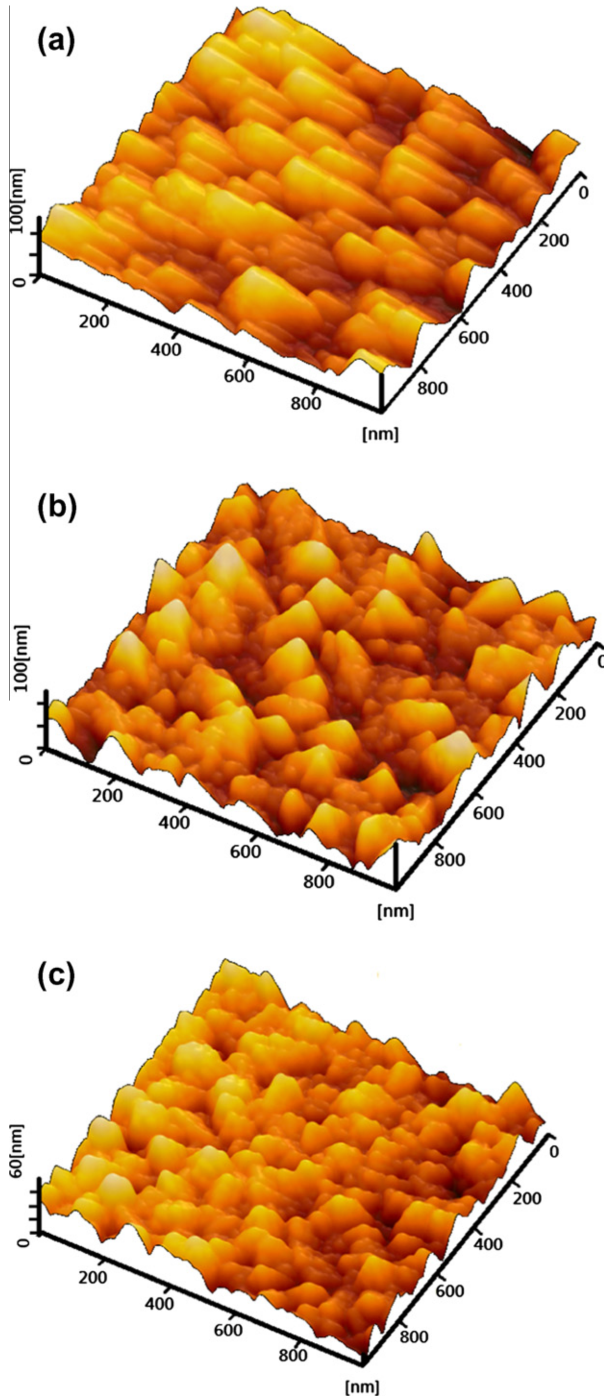

Fig. 7. AFM images of the TiO_2 films with different sputtering process parameters (a) $A_1B_1C_1D_1$, Ra = 1.9 nm, (b) $A_2B_1C_2D_3$, Ra = 16.7 nm, (c) $A_3B_1C_3D_2$, Ra = 14.1 nm (d) $A_1B_3C_3D_3$ (optimal deposition condition), Ra = 12.3, respectively.

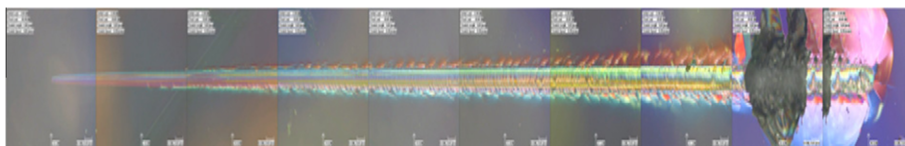

Fig. 8. The scratch test of the TiO_2 film grown onto non-alkali glass substrates.

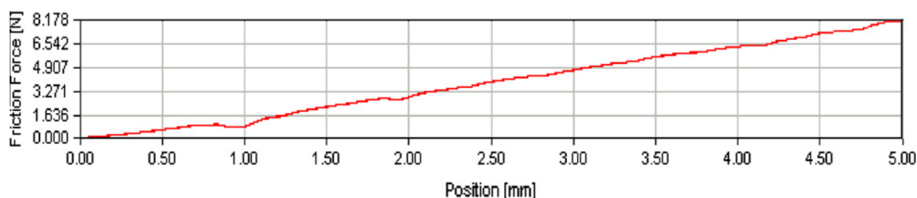

Fig. 9. The frictional force vs. position in the scratch test.

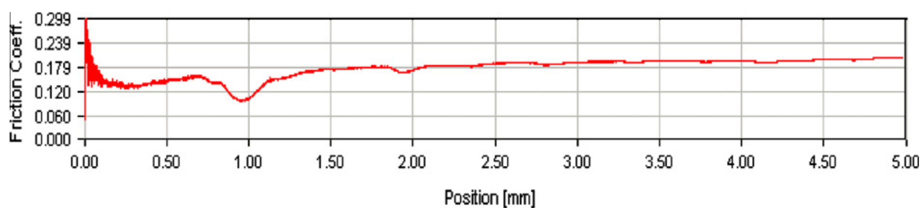

Fig. 10. The friction coefficient vs. position in the scratch test.

solution, degraded by TiO_2 photocatalytic film, for orthogonal arrays No. 1–9 and the optimal deposition condition ($A_1B_3C_3D_3$), after 4 h of UV irradiation. These experimental conditions ($A_1B_3C_3D_3$) were used for three consecutive experiments. The confirmation runs show that the lowest absorbance of MB, 0.26, was obtained for the optimal deposition conditions ($A_1B_3C_3D_3$), so the Taguchi method produced an improvement in MB photodecomposition.

The photo-induced hydrophilicity of the TiO_2 thin films was evaluated by measuring the contact angles to pure water droplets, during irradiation with UV, as shown in Fig.4. It can be seen that the contact angle decreases as the UV irradiation time increases. The initial water contact angles of the TiO_2 films range from 61.85° to 12.95°, but when the film surface is irradiated by UV light, the water contact angle begins to decrease, i.e. photoinduced hydrophilicity increases. After UV irradiation for 9.0 min, all of the water contact angles are below 45°, which means that the TiO_2 films exhibit good photo-induced hydrophilicity. The contact angle of the TiO_2 thin film, deposited using the sputtering process parameter set, $A_1B_3C_3D_3$ (optimal deposition condition), decreased from 55° to less than 7°, after UV irradiation for 3.0 min, which demonstrates a significant hydrophilic effect. For the TiO_2 thin film deposited using the sputtering process parameter set, $A_1B_1C_1D_1$ (No.1), the contact angles decrease from 55° to 45°, during 9.0 min of UV illumination, which shows that the surface of the film is less hydrophilic. The contact angle of the glass substrate does not decrease, even after the UV irradiation for 240 min, so the glass substrate demonstrates no hydrophilic characteristics.

The photocatalytic characteristics of TiO_2 materials depend heavily upon surface morphology, crystal structure and crystallization of the TiO_2 photocatalyst [21]. Fig. 5 shows the X-ray diffraction patterns of the TiO_2 films deposited on non-alkali glass, for L_9 orthogonal arrays No. 1–9, and using $A_1B_3C_3D_3$ (optimal deposition conditions). High substrate temperature results in good crystalline structure, whereas low substrate temperature leads to an amorphous TiO_2 structure [22]. The films deposited using $A_1B_1C_1D_1$ (No. 1, smaller dc power and lower substrate temperature) exhibited an

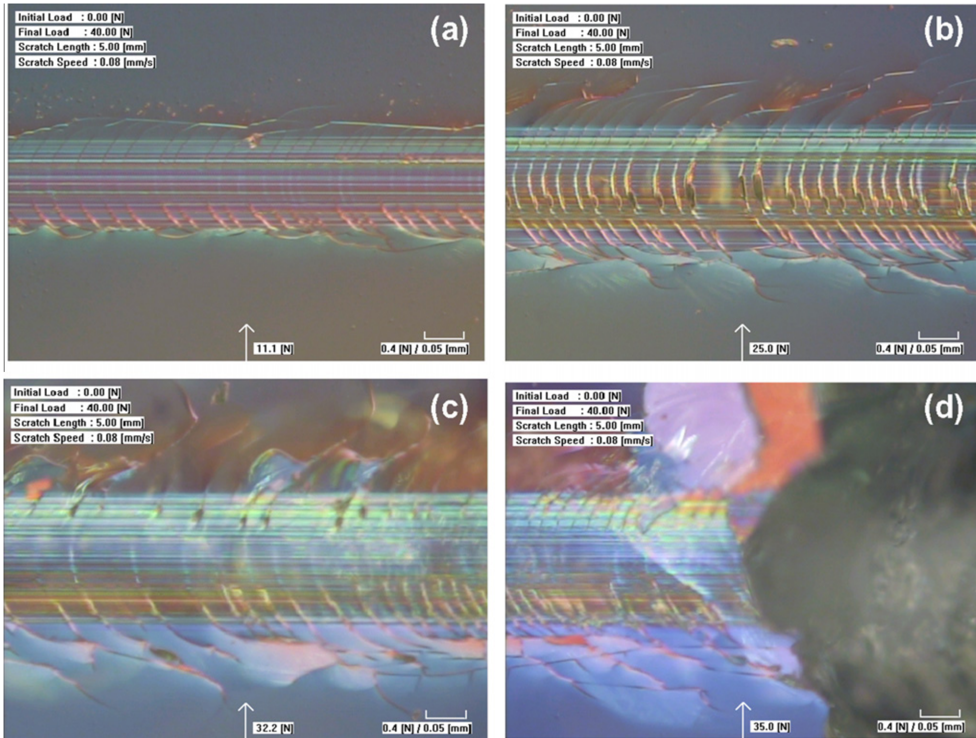

Fig. 11. The microscopic observations of the TiO_2 film to substrate with normal loads (a) 11 N, (b) 25 N, (c) 32.2 N and (d) 35 N. respectively.

amorphous structure. The TiO_2 film deposited under the optimal deposition conditions ($A_1B_3C_3D_3$) exhibited a mixture phases of anatase (2 0 0) and rutile (1 1 0) and (2 0 0) diffraction peaks, which demonstrate a higher crystallinity than the other films.

The surface morphology of the TiO_2 films was examined, using SEM and AFM. Fig. 6 shows the SEM micrographs of the TiO_2 films, deposited with different sets of process parameter. The thickness of the thin films obtained with parameter sets, $A_2B_1C_2D_3$ (No.4), $A_3B_1C_3D_2$ (No. 7) and $A_1B_3C_3D_3$ (optimal deposition conditions), were approximately 822.6, 702.0 and 437.4 nm, respectively. The sizes of these particles were not equal, even within the same film. It can be seen that the film deposited at a higher substrate temperature contains more spherical particles and an almost homogenous structure, and the grain sizes are relatively small (Fig. 6c). The smaller nano-crystalline TiO_2, with nano-sized holes, provides more surface area for the photocatalytic process than films with an amorphous structure, or films with large grain sizes [19]. The exciton energy of the nanoparticles is estimated using the Brus equation, i.e., the effective mass model (EMM) [23,24] :

$$\Delta E_g = \frac{h^2}{8R^2\mu} - \frac{1.8e^2}{\varepsilon R} \tag{1}$$

where ΔE_g is the band gap shift, R is the radius of the particle size, μ is the reduced mass of the exciton and ε is the dielectric constant. The band gap of ultra-fine semiconductor particles increases, as particle size decreases, when it is less than the minimum band gap. This result agrees with the experimental results of Lin et al. [25], who showed that the smaller the particle size, the faster is the rate of degradation.

Fig. 7 shows the AFM images and root mean square (rms) surface roughness of the grown films, for different deposition conditions. It can be seen that the film is crack-free and smooth. The rms roughness of the films varies from 12.3 to 16.7 nm. The morphology of the TiO_2 film deposited under optimal conditions exhibits slightly smooth and small grains, compared with those produced using other deposition conditions.

The adhesion of the TiO_2 film was determined by a scratch test, the most widely accepted measurement technique for the adhesion of hard, thin coatings. Fig. 8 shows a microscopic image of a diamond stylus traversing the surface of the TiO_2 coating deposited under optimal conditions. It travels at 0.08 mm/s and the normal load is increased, every 5 mm, from 0 to 40 N. The fictional force was continuously recorded, during the scratch test. Fig. 9 shows that the frictional force is almost proportional to the position, along the scratch. Fig. 10 shows a plot of the calculated coefficient of friction, between the coating and the stylus, vs. the position along the scratch. There is transient vibration, at the initial position, and an undesirable response, at 0.9 mm. The coefficient of friction remains almost constant, at 0.18, after 1.5 mm, which implies that the frictional force is not affected by defects in the glass. The microscopic images of the TiO_2 film to substrate, with normal loads (a) 11 N, (b) 25 N, (c) 32.2 N and (d) 35 N, are shown in Fig. 11. Under a normal load of 11 N, there are no scratch failures, including cracks, tearing, or flaking, in the scratch channel. Under normal loads of 25 and 32.2 N, shown in Figs. 11(b) and (c), respectively, the TiO_2 film remains on the substrate, although some cracks exist, in the substrate. Another typical failure, under a normal load of 35 N, shown in Fig. 11(d), begins with conformal cracking of the substrate, followed by gross spallation, but there is no failure of adhesion of the TiO_2 film to the substrate. The scratch test indicates that the TiO_2 films exhibit excellent adhesion. The films are very compact and homogeneous and they adhere to the substrate.

4. Conclusions

TiO_2 thin films were deposited on non-alkali glass substrates, using dc magnetron sputtering, with a ceramic TiO_2 target, in an argon gas environment. This study used a Taguchi experimental design to determine the influence of various deposition process parameters on the photocatalytic activity of TiO_2 films. The substrate temperature was found to have the major affect on MB absorbance, and the deposition time and sputtering pressure ranked second and third, respectively. An optimal parameter set, $A_1B_3C_3D_3$ (90 W dc power, 2 Pa sputtering pressure, 500 °C substrate temperature, 180 min deposition time) improved the photocatalytic characteristics of the TiO_2 films and produced a film with a mixture phases, with anatase (2 0 0) and rutile (1 1 0) and (2 0 0) diffraction peaks. This film exhibited higher crystallinity than the other films. It can be seen that the film deposited using optimal parameter settings contains more spherical particles and has an almost homogenous structure, with relatively small grain size. The scratch test indicates that the TiO_2 films exhibit excellent adhesion. The experimental results illustrate the effectiveness of this approach.

References

[1] L. Chen, M.E. Graham, G. Li, K.A. Gray, Thin Solid Films 515 (2006) 1176.
[2] Q. Xiao, L. Ouyang, Chem. Eng. J. 148 (2009) 248.
[3] O. Carp, C.L. Huisman, A. Reller, Prog. Solid State Chem. 32 (2004) 33.
[4] Z.Y. Chen, Y. Hu, T.C. Liu, C.L. Huang, T.S. Jeng, Thin Solid Films 517 (2009) 4998.
[5] J. Wang, S. Uma, K.J. Klabunde, Appl. Catal. B 48 (2004) 151.
[6] C.H. Huang, C.C. Tsao, C.Y. Hsu, Ceram. Int. 37 (2011) 2781.
[7] L. Sirghi, T. Aoki, Y. Hatanaka, Thin Solid Films 422 (2002) 55.
[8] S. Ohno, N. Takasawa, Y. Sato, M. Yoshikawa, K. Suzuki, P. Frach, Y. Shigesato, Thin Solid Films 496 (2006) 126.
[9] K. Eufinger, D. Poelman, H. Poelman, R. De Gryse, G.B. Marin, Appl. Surf. Sci. 254 (2007) 148.
[10] J. Šícha, J. Musil, M. Meissner, R. Čerstvý, Appl. Surf. Sci. 254 (2008) 3793.
[11] Y.M. Sung, H.J. Kim, Thin Solid Films 515 (2007) 515.
[12] W.S. Lin, C.H. Huang, W.J. Yang, C.Y. Hsu, K.H. Hou, Curr. Appl. Phys. 10 (2010) 1461.
[13] B. Liu, X. Zhao, Q. Zhao, C. Li, X. He, Mater. Chem. Phys. 90 (2005) 207.
[14] C.C. Chen, W.J. Yang, C.Y. Hsu, Superlattices Microstruct. 46 (2009) 461.
[15] G. Taguchi, S. Chowdhury, Y. Wu, Taguchi's Quality Engineering Handbook, John Wiley & Sons Hoboken, NJ, 2005.
[16] C.Y. Hsu, Y.Y. Lin, W.S. Lee, S.P. Lo, J. Mater. Process. Technol. 198 (2008) 359.
[17] J. Szczyrbowski, G. Brauer, M. Ruske, G. Teschner, A. Zmelty, J. Non-Cryst. Solids 218 (1997) 262.
[18] H. Ohsaki, Y. Tachibana, A. Mitsui, T. Kamiyama, Y. Hayashi, Thin Solid Films 392 (2001) 169.

[19] H. Tomaszewski, H. Poelman, D. Depla, D. Poelman, R. De Gryse, L. Fiermans, M.F. Reyniers, G. Heynderickx, G.B. Marin, Vacuum 68 (2003) 31.
[20] S. Flickyngerova, K. Shtereva, V. Stenova, D. Hasko, I. Novotny, V. Tvarozek, P. Sutta, E. Vavrinsky, Appl. Surf. Sci. 254 (2008) 3643.
[21] H. Ogawa, T. Higuchi, A. Nakamura, S. Tokita, D. Miyazaki, T. Hattori, T. Tsukamoto, J. Alloy Compd. 449 (2008) 375.
[22] W. Zhang, Y. Li, S. Zhu, F. Wang, Surf. Coat. Techol. 182 (2004) 192.
[23] L.E. Brus, J. Chem. Phys. 79 (1983) 5566.
[24] L.E. Brus, J. Chem. Phys. 80 (1984) 4403.
[25] H. Lin, C.P. Huang, W. Li, C. Ni, S.I. Shah, Y.H. Tseng, Appl. Catal. B 68 (2006) 1.